NASA TECHNICAL NOTE

NASA TN D-5137

c. 1

NASA TN D-5137

TECH LIBRARY KAFB, NM
0131885

LOAN COPY: RETURN TO
AFWL (WLIL-2)
KIRTLAND AFB, N MEX

SUPERCONDUCTIVE DUST CORES FOR INDUCTIVE ELEMENTS

by Russell J. Jirberg

Lewis Research Center

Cleveland, Ohio

NATIONAL AERONAUTICS AND SPACE ADMINISTRATION • WASHINGTON, D. C. • APRIL 1969

TECH LIBRARY KAFB, NM
0131885

NASA TN D-5137

SUPERCONDUCTIVE DUST CORES FOR INDUCTIVE ELEMENTS

By Russell J. Jirberg

Lewis Research Center
Cleveland, Ohio

NATIONAL AERONAUTICS AND SPACE ADMINISTRATION

For sale by the Clearinghouse for Federal Scientific and Technical Information
Springfield, Virginia 22151 – CFSTI price $3.00

ABSTRACT

The use of superconductive dust as a core filler for inductive coils was investigated as a means of producing magnetically variable inductive elements. Both lead and niobium-filled cores were studied in static background magnetic fields. The observed inductance variations and the origin of alternating-current losses are discussed in relation to their superconducting properties.

SUPERCONDUCTIVE DUST CORES FOR INDUCTIVE ELEMENTS

by Russell J. Jirberg

Lewis Research Center

SUMMARY

The impedances of coils with superconductive dust cores composed of -325 mesh powders of lead and of niobium were measured in dc background magnetic fields. These tests demonstrate the ability of the dust cores to produce magnetically variable inductances suitable for high-frequency operation.

The inductances vary in direct proportion to the normal volume within the cores. The field dependence is shown to be a result of the filamentary magnetic structure of the superconductors. Unique behavioral qualities of the two cores are related to the value of their Ginzburg-Landau κ parameter.

The resistive components of the impedances indicated the existence of two distinct "superconducting" alternating-current loss mechanisms. One is a joule heating by the shielding currents induced in the superconducting-normal matrix of the filamentary microstructure. The second (observed only in the niobium) is a hysteretic loss which occurs in type II superconductors subjected to alternating-current fields. Throughout the entire field range below H_{c2} this loss is shown to vary directly with the cube of the modulating field and inversely with the critical current density, as is predicted by the Bean-London theory.

INTRODUCTION

The unique properties of the superconducting state have stimulated the development of many new types of electronic control and memory devices. The most notable development in this area must certainly be the cryotron. Other examples, however, would include superconducting bolometers, transmission lines, microwave cavities, high Q resonant circuits, and variable inductance elements.

Of the latter type several basic forms have evolved. In particular, Slade (ref. 1) described a variable inductance element using a solenoidal coil on a core of high permeability jacketed by a superconductive sheath. A background magnetic field is used to

switch the superconductive jacket between its superconducting and normal states. As the jacket switches states the permeability of the total core changes between a perfectly diamagnetic state (or nearly so) to one of high permeability. The transition increases the ability of the core to contain the flux. Hence, the total magnetic energy in the core increases. The result is a step increase in the inductance of the coil.

A similar device in thin film form was devised by Cassidy and Meyerhoff (ref. 2). In this instance the inductance of a strip conductor is controlled by the diamagnetic shielding of a nearby superconducting plane. Thin film construction was also used in a device called the ryotron described by Grange (ref. 3) and by Miller, et al. (ref. 4). In contrast with the Cassidy-Meyerhoff device which uses an externally generated magnetic field to drive the superconducting ground plane normal, the ryotron uses a current in the shielding element to effect the switching.

Each of these devices is, of course, a variation on the same theme. In each the inductance is altered by the expulsion of magnetic flux from regions where it might otherwise exist. And each device functions essentially as a switch, "toggling" between its available states through the action of the control field or current. However, for each there exist limitations on its switching speed or maximum driving frequency. These arise in two ways. One is due to the large capacitive coupling between the coil and core. The other is due to excessive I^2R losses of the eddy currents induced in the control elements. Both are particularly serious effects in the Slade device with its sluglike metal core.

These drawbacks aside, the use of superconducting materials to produce magnetically variable inductances remains an attractive concept. But to realize a useful inductive element for audiofrequencies or radiofrequencies requires that these detrimental effects be reduced or eliminated. Inductance values appropriate to these frequencies range from microhenries to millihenries or higher - a range not readily attained by thin film techniques. Therefore, it would seem that the solenoidal coil adopted by Slade, or alternatively a toroidal configuration, should be retained. The solution thus lies in the proper design of the core.

Described herein is one approach to the problem. As in the Slade device, the inductance is varied by altering the magnetic shielding of core volume. But the shortcomings of the Slade device are avoided by distributing the superconductor throughout the core in a finely divided form in an insulating matrix. This is a ploy similar to the use of ferrites rather than iron cores for ordinary radiofrequency coils. In operation, the superconducting regions within the core electrically "remove" volume from the core. The result is a reduction in the capacity of the coil to store magnetic energy. Consequently, the inductance of the coil is reduced from the value it assumes with a totally permeating field. The extent of the reduction will be shown to depend directly on the fractional volume of superconductor in the core. Between these extremes the inductance may be

varied by control of the ambient magnetic field.

This report examines the behavior observed in two different cores, one filled with type I superconducting lead powder, the other with type II superconducting niobium powder. Emphasis is placed on relating the field dependence of the inductance and the losses to the structure of the superconducting state and to the nature of the field penetration. It is not the objective of this report to exhaustively study the device capabilities of a superconductive duct core, variable inductance element. Rather the aim is to develop an understanding of the cores' responses based on the fundamental properties of superconductors. In addition, limitations inherent to the dust cores, particularly as regards the alternating-current losses, are also sought.

EXPERIMENTAL PROCEDURES

Test Samples

To understand how the cores function requires that the various factors affecting the impedance be isolated. Except under the most favorable circumstances, separating the effects of currents set up in the core and coil as well as nearby conducting surfaces is a formidable task. Necessarily then a coil-core configuration of the simplest geometry was chosen to facilitate the task. The inductance coils used in these tests consisted of single layer close-wound solenoids tightly wrapped around cylindrical cores. This type of coil is readily handled by standard inductance formulae supplemented with tabulated corrections for end effects and winding pitch (ref. 5).

The cores were cylindrical slugs of commercially available micron-sized (-325 mesh) superconductive metals dispersed in an epoxy matrix. The epoxy served both to insulate the metal particles one from another, and to bind them together. Surrounding, and coaxial with the coils, were placed copper cylindrical electrostatic shields. The shields, coils, and cores were mounted on a conventional UHF jack (type SO-239). This provided a convenient means of connecting to the coil assemblies and suspending them in the liquid helium and the magnetic field. Shown in figure 1 is the lead coil-core assembly with the shield removed.

Cores

The core samples were prepared from -325 mesh powders of 99.9999 percent purity lead and 99.5 percent purity niobium. The particle sizes were measured with a comparison microscope. Figures 2 and 3 indicate the size distribution of the two powders. The jagged shape of the individual particles is also shown in the photomicrograph inserts.

A commercially available epoxy was the dispersing medium. Its low viscosity (5 to 7 P at room temperature) permitted the epoxy to be heavily and quickly loaded with the metal powders by a simple stirring action. To retain the low viscosity of the resin, diethylene triamine was used as the curing agent. The dispersions were molded in glass test tubes lightly greased with a silicone release agent. Air bubbles introduced by the stirring were removed by reducing the pressure above the epoxy. Upon curing, the samples were cut into right circular cylinders with an abrasive saw and removed from their glass encasements. An unloaded epoxy sample was similarly prepared for use as a control sample.

The filling factors (i. e., the ratio of powder volume to total core volume) were derived from their densities. Each is listed in table I along with the densities of the corresponding metal-epoxy composite and the unloaded epoxy. The lead-filled sample is

TABLE I. - FILLING FACTORS OF TEST

SAMPLE CORES

Sample	Sample	Metal	Epoxy	Filling factor
	Specific gravity			
Pb-815	5.83	11.35	1.17	0.460
Nb-815	3.56	8.589	1.17	.322

designated as Pb-815, the niobium-filled one as Nb-815. Reported densities (refs. 6 and 7) of the metals in the bulk were used in calculating the filling factors. Since the densities quoted by various sources vary by almost 2 percent, and since the actual densities of the metals used could not be determined, the filling factors may be in error by about 2 percent.

Sample Coils and Shields

A coil of 48 turns of number 34 gage enameled wire was centered on the lead-filled slug. The windings were close-wound and tightly wrapped onto the slug and secured in place with clear epoxy. The slug extended roughly 1 diameter beyond each end of the coil. After preliminary inductance measurements, a cylindrical copper shield (0.25 mm wall thickness) was affixed to the supporting UHF connector. The need for such a shield arose in order that conducting surfaces in close proximity to the coils be of high conductivity so as not to resistively load the coils. Without it the thin silver heat shield of the

Dewar in which the coils were immersed during testing would have loaded the coils too heavily. The size of the shield was dictated by the limited space available in the testing Dewar. The shield had a diameter roughly twice that of the coil, and extended approximately two coil diameters beyond each end of the coil. Holes in the shield near the connector allowed a free flow of liquid helium around the coil and core.

The construction of the niobium-filled sample was identical with one exception. The coil, $20\frac{1}{2}$ turns of number 24 gage Nyclad copper wire, was made self-supporting. This enabled the core to be slipped in and out of the coil without distorting it. This capability aided in isolating the various sources of the radiofrequency losses, a point that will be discussed later.

The pertinent parameters for both samples are listed in table II. The unshielded

TABLE II. - TEST COIL PARAMETERS

Parameter	Sample	
	Pb-815	Nb-815
Diameter of coil, d_w, cm	0.843	0.873
Diameter of insulated wire, cm	0.0175	0.0554
Diameter of bare wire, cm	0.0160	0.0503
Axial length of coil, l_w, cm	0.853	1.11
Number of turns, N	48	20.5
Diameter of shield, d_s, cm	1.71	1.71
Diameter of core, cm	0.826	0.818
Unshielded inductance, μH:		
Calculated	12.9	2.02
Measured	13.0	2.03
Mutual coupling coefficient:		
Calculated	0.137	0.165
Measured	0.136	0.158
Shielded inductance, μH:		
Calculated	11.1	1.68
Measured	11.2	1.71

inductances were calculated using formulae for the inductance of an equivalent current sheet, including corrections for end effects and finite winding pitch. This is a standard procedure outlined in many texts including an especially comprehensive one by Grover (ref. 5). The shielded inductances were calculated using the coefficient of mutual coupling determined from a semiempirical relation developed by Bogle (ref. 8). Room temperature measurements of both the unshielded and the shielded inductances are in good agreement with the calculated values. The details of the measurement technique are given in the next section.

Impedance Measuring Techniques

As already indicated, the principal function of the superconducting dust is to diamagnetically shield portions of the core. But equally important is the response of the core particles to the ac field while in the normally conducting state. To realize the greatest variation of inductance between the totally normal and the totally superconducting states, the core particles must appear to be magnetically "transparent" while in the normal state. This is in contrast to their being magnetically "opaque" while in the superconducting state. Transparency, in the sense that the ac magnetic field is insignificantly attenuated within the particles, prevails when the particles are small in comparison with the skin depth. The opposite situation, opacity, prevails when the particles are large compared to the skin depth. In that case, the oscillatory field is essentially locked out of all but the surface. Therefore, in order that the ac field effectively penetrate the particles in the normal state, the frequency must be kept below that at which the skin depth approaches the size of the particle.

With this restriction in mind the selection of a testing frequency was based on the conductivity and dimensions of the particles to be tested. For the -325 mesh niobium powder, 3588 kilohertz could be used from 300 to 4.2 K. For the -325 mesh lead powder, however, this frequency resulted in an unfavorable skin depth to particle size ratio at 4.2 K to the higher resistivity ratio of the lead. The measurements of the lead-filled sample at 4.2 K were thus restricted to 10 kilohertz to accommodate its higher conductivity. Hence, in both cases the radiofrequency skin depths were made to be far greater than the largest particle diameter; an effective test of the superconductive influence of the core particles is thereby assured.

High-Frequency Apparatus

At 3588 kilohertz the equivalent parallel reactive and resistive impedance components were simultaneously extracted using a radiofrequency impedance bridge. As schematically indicated in figure 4, the coil assembly was suspended in the liquid helium Dewar and connected to the bridge through a coaxial transmission line (RG-63/U). In order to take full advantage of the accuracy of the bridge, the frequency of the oscillator was continually monitored with the counter and maintained constant. (Frequency varied by less than 0.003 percent.) The communications receiver served as a null detector for the bridge. By displaying the audio beat frequency generated in the receiver on an oscilloscope, the null balance condition could be determined with great sensitivity.

The background magnetic field was supplied by a conventional iron core electromagnet. The field could be set to within 0.2 percent of a desired value and was uniform

to within 10 parts per million over the core region. A provision for reversal of the field permitted the samples to be examined for possible flux trapping effects.

Since it was necessary to locate the sample coil away from the bridge (~1 m), its impedance is perturbed by the intervening coaxial cable. The actual impedance components may be calculated from those seen at the bridge by a procedure outlined in appendix A. The treatment shows that a knowledge of only the shorted and the open-ended impedances of the transmission line at the test frequency is needed to correct for the effect of the transmission line.

By supplying the bridge with a source of constant amplitude radiofrequency voltage, the impedance under test is subjected to a likewise constant amplitude driving voltage. With high Q (i.e., low loss) impedances as measured in these tests, this forces the amplitude of the driving current to vary inversely with the inductive component of the impedance since it is by far the dominant component. Consequently, the radiofrequency field varies inversely with the inductance. In these tests the niobium-filled core was subjected to a radiofrequency field of between 0.7×10^{-6} and 1.1×10^{-6} tesla (7 and 11 mG) in amplitude.

10 Kilohertz Apparatus

The measurements made at 10 kilohertz differed from those mentioned previously in that a bridge with a self-contained oscillator and detector was used. A 10-kilohertz current, derived from the oscillator and constant in amplitude to within 1 percent, was cabled to the sample coil through a length of RG-174/U coaxial line. The voltage developed across the sample coil was returned to the bridge through a separate coaxial cable. The resistive and inductive components of the impedance were obtained from the corresponding verniers of the bridge balance controls. (The bridge is calibrated in terms of the effective series resistance and inductance of the unknown to within an accuracy of 0.25 percent.) Impedance components obtained from the dial readings were corrected for the influence of the coaxial cable and connector by prezeroing the bridge with the sample coil assembly replaced by a shorting plug.

With a 5-milliampere amplitude current driving the sample coil, the alternating-current field produced in the core was approximately 35×10^{-6} tesla (350 mG). Since in this case the driving current was constant in amplitude, the ac field thereby generated was also constant.

As in the tests on the niobium sample, the background field was transverse to the coil axis. In both cases, data was obtained in both increasing and decreasing field sequences.

RESULTS AND DISCUSSION

Displayed in figures 5 and 6 are the field dependent impedances of the two sample coils. Each shows a general rise of the inductance with increasing field strength. The specific manner, however, in which the inductances vary with the applied field is different. Also different are the power losses as reflected by the resistive components. In the discussion that follows, the bases for these behaviors and the differences between them will be shown to originate in the nature of the field penetration peculiar to the two types of superconductors.

Basic to a discussion of these results is a recognition of the fact that an external magnetic field will, in general, permeate a superconducting body. Only fields that do not exceed a value set by the demagnetizing coefficient of the body and its critical field are shielded from its interior. Otherwise, the field penetrates the body forming a magnetic substructure within. Depending on the class of material (type I or type II superconductor), one of two types of structures is formed.

In a type I superconductor a laminar or sponge structure of normally conducting regions imbedded in the superconducting regions occurs. The field penetrates the body by threading through the normal regions. This is the "intermediate" state. On the other hand, a type II superconductor assumes a very fine structured state of normal filaments within a superconducting matrix. Here the field penetration takes place on the flux quantum level. This is the "mixed" state.

In either case, an increase in the external field causes a growth in size or number of the normal filaments at the expense of the superconducting component. It is on the basis of the formation of this magnetic microstructure that the superconducting particles of the dust cores can, in part, support an ac flux. The general inductance rise with field strength follows directly from the increase in normal regions within the core particles. Moreover, every feature of the cores' responses can be consistently explained within the framework of these magnetic substructure models.

Superconducting Filling Factor

That the essential features of the impedance components are consequences of superconducting filamentary structures can indeed be demonstrated. To that end, it is useful to develop first a relation between the coil inductance and a somewhat artificial quantity termed the effective superconducting filling factor. The filling factor is defined as the ratio of superconducting volume to total volume in the core. It thereby specifies the fractional volume of the core that experiences perfect diamagnetic shielding. Since the test frequencies were chosen so that the normal skin depths were well in excess of the

particle sizes, diamagnetic shielding via normal eddy currents is feeble. Effectively, then only supercurrent shielding has any relevance. The filling factor thus may be obtained from the inductance on the basis of their interrelation through the shielding.

Basically, the inductance of a coil is defined through an energy expression as

$$L = \frac{2W_m}{I^2} \tag{1}$$

where W_m is the magnetic energy of the field generated by the current I in the coil. In turn, the magnetic energy may be expressed in terms of the field by the volume integral

$$W_m = \frac{1}{2} \int_V B \cdot H \, dV \tag{2}$$

where H is the magnetizing force and B is the resulting flux density. Thus, it is easily seen that those regions where $B = 0$ by virtue of perfect diamagnetic shielding contribute nothing to the inductance. In the superconductive dust cores, then, that volume occupied by actual superconducting material is, in effect, removed from the core. Accordingly, the inductance is reduced. By applying a background field of sufficient strength to bring the superconductive material into either the intermediate state (for a type I) or the mixed state (for a type II), the superconducting filling factor may be varied. The background field serves to control that volume which contributes to the inductance.

With the particles being so small and uniformly distributed throughout the core, the overall distortion of the ac flux lines in the core is slight. Essentially, one can consider the ac flux modified only to the extent that its total quantity is reduced in proportion to the superconducting filling factor. The coil inductance may thus be written as

$$L_w(\sigma) = L_w(0)(1 - \sigma) \tag{3}$$

Here, σ is the field-dependent effective superconducting filling factor, and $L_w(0)$ is the intrinsic inductance of the coil when $\sigma = 0$.

The shielding by the core particles affects not only the inductance of the coil, but also the extent to which the surrounding shield perturbs the impedance of the coil-shield combination. Currents induced in the shield are, in general, out of phase with the driving current in the coil. The phase shift is determined by the conducting properties of the shield. The effect of an induced current in the shield is both to reduce the apparent inductance of the coil, and to impose an additional component on the resistive or loss

term. Hence, impedance measurements made on a shielded coil require appropriate consideration of the influence of the shield.

Since the coil and shield are inductively coupled, the combination resembles a transformer with a shorted single turn secondary. An analysis of the shielded coil can thus be made based on the equivalent circuit for such a shorted transformer. The details of the analysis are given in appendix B. Presented in figures 5(a) and 6(a) are the inductances of the sample assemblies with the modifying influence of the coaxial cable removed as described in appendix A. From these inductance values, the superconducting filling factors of figures 5(c) and 6(c) were calculated as described in appendix B.

In the high field limit the measured inductances are in agreement with values derived solely from the coil geometries (see table II). The calculations assume a core permeability equal to that of vacuum. This indicates that radiofrequency shielding by the normal state core particles is truly negligible at these frequencies. At low background fields the inductances are reduced in direct correspondence to the actual fractional superconductive volume in the core: The values of σ obtained from the inductance curves at $H = 0$ (i. e., the totally superconducting state) are in excellent agreement with the volumetrically determined values (see table I, p. 4). Hence, as proposed, the essential role of the superconductor is one of varying the inductance of the coil by "removal" of volume from within the core.

Beyond this point of common behavior, the two samples differ markedly. The behavior of each, however, can be understood in terms of the properties of its class of superconductor. In this regard, the chief distinction is the manner in which the field penetrates the superconductor.

Lead Core

Lead, being a type I superconductor, completes its transition to the normal state in an increasing background field at 0.054 tesla (540 G), the bulk critical field at 4.2 K. The saturation of the inductance at 0.054 tesla (see fig. 5(a)) demonstrates this fact. The inductance does not, however, change abruptly at the bulk critical field. Instead, there is a gradual rise in inductance preceding the final transition. The effect is due to the formation of the intermediate state. This is seen as follows.

In each powder particle the background field induces the intermediate state at a field value dependent on the demagnetizing coefficient of the particle. Due to the jagged shape of the particles the intermediate state undoubtedly is induced throughout the sample at very low values of the field. Since the field penetrates in the intermediate state forming some sort of filamentary structure, the core becomes a myriad of multiply connected superconducting regions at fields far below the bulk critical field.

These regions constitute a network capable of supporting lossless circumferential

shielding currents. As such they prohibit the penetration of the ac field into the particles. Upon raising the dc field, though, more and more normal regions are accommodated into the structure, and the superconducting network approaches a critical point. At this point the multiply connected supercurrent network begins to dissolve. Those segments of the superconducting network perpendicular to the dc field are the weak links in the network since the critical current density is lowest for their orientation. As the last of these segments are driven normal, the superconducting network that supports the circumferential shielding currents is broken, and the ac field begins to penetrate the particle. It is significant that the first penetration of the ac field (as indicated by the first change of inductance) occurs at a dc field value equal to one-half that of the bulk critical field. Apparently, the crucial segments of the superconducting network had been reduced essentially to cylindrical filaments prior to the ac field penetration. (The demagnetizing coefficient for a cylinder with its axis at right angles to the field direction (ref. 9) has the value 0.5.)

The dissolution of the multiply connected aspect of the particles is also marked by increased power dissipation in the sample. This is reflected by a rise in the resistive component of the impedance. At low fields, where the shielding currents in the core particles are totally superconducted, the only significant power losses occur in the coil windings and in the copper shield. The power loss, therefore, is constant until the network supporting the supercurrents begins to dissipate. Thereafter, the shielding currents are driven in part through normally resistive regions. As the dc field is further increased, the average resistivity to eddy currents in the partially superconducting material rises, and a rise in the resistive impedance component occurs. This increase in power dissipation continues until the ac flux nears saturation. Then, as the last remaining superconducting regions are driven normal, the further increases in the average resistivity serve to decrease the eddy currents. This, in turn, causes a decrease in the power dissipation. The power dissipation thus reaches a maximum and subsequently drops to a value determined by the resistivity of the totally normal metal. The broad peak observed in the resistance component shown in figure 5(b) stems from just such a penetration of ac flux into a medium of variable conductivity. Because of the complex interplay of currents in the sample assembly, it was not possible to determine a functional dependence of the resistance on field. Qualitatively, however, the behavior is understandable.

A rather unusual feature of the lead-filled sample is its different responses to increasing and decreasing dc fields. This hysteresis-like behavior results from the formation of a metastable surface state. St. James and deGennes (ref. 10) theorized that the normal phase in a superconductive body may supercool (in a field sense) below the thermodynamic critical field H_c to H_{c3}:

$$H_{c3} = C\sqrt{2}\ \kappa H_c \tag{4}$$

where κ is the Ginsburg-Landau parameter. The coefficient C allows for the variation of H_{c3} with the angle of incidence between the field and the surface; C varies monotonically from 1.695 for the parallel situation to 1 for the field normal to the surface.

Originally, it was held that at H_{c3} the superconducting phase nucleates on the surface of the body and immediately spreads throughout its bulk. Recently, however, Feder (ref. 11), Park (ref. 12), and McEvoy, et al. (ref. 13) have shown for materials with κ between 0.406 and 0.595 that, although the superconducting phase nucleates at H_{c3}, the surface sheath actually supercools to a field H_s, where $H_s < H_c$, before a first-order transition to the Meissner state occurs. Only for materials with $\kappa < 0.406$ is $H_s = H_{c3}$. For κ between 0.595 and 0.707, the transition to the superconducting state occurs at H_c. Above 0.707, of course, is the realm of type II superconductivity.

The fact that the inductance attains its maximum value (indicating complete ac flux penetration) in an increasing dc field at precisely the bulk critical field value assures that $H_{c3} < H_c$ for this lead. It can thus be argued that the field to which the lead actually supercools is indeed H_{c3}. Furthermore, it can be shown that the degree of supercooling is in accordance with the known κ value for lead. This can be done as follows.

The applied dc field at which a given segment of the superconducting network undergoes the phase transition is determined by its demagnetizing coefficient. This is dictated by its shape and orientation in the field. The first filaments to suffer the transition are seen to be those with demagnetizing coefficients of very nearly 0.5. The last to make the transition are those with zero demagnetizing coefficient. With the coefficient equal to zero, the applied field is uniformly parallel to the surface of the segment. In that case, the applied field at the point of transition is exactly equal to the critical field. Therefore, taking 0.051 tesla as the supercooling field H_s as evident in figure 5(a), the supercooling field ratio H_s/H_c is 0.95. According to reference 13 this assures $H_{c3} = H_s = 0.051$ tesla (510 G).

That being the case, one can calculate κ from the expression for H_{c3} given by equation (4). Recalling the coefficient C to be 1.695 when the applied field is parallel to the surface, one obtains $\kappa = 0.39$. By comparison, Strongin, et al. (ref. 14) claim $\kappa = 0.38 \pm 0.05$ for pure lead at 4.2 K.

As the field is decreased below 0.051 tesla, the superconducting state still nucleates in a region at a local field value of H_{c3}, but in an applied field reduced by the demagnetizing coefficient of the region. Thus, the response of the sample in decreasing dc fields lags that in increasing fields until total shielding is once again restored at one-half of the bulk critical field.

Reducing the applied dc field to zero and raising it again in a reversed sense gave

no indication of flux trapping. The sample's response was the same for either direction. Modulating the applied field about some field value where the ac flux partially penetrates the particles causes the inductance and resistance to trace out minor hysteresis-like loops. Each vaies within an envelope established by the response curves shown in figure 5.

Niobium Core

For the niobium-filled sample (fig. 6) the ac field penetrates the core over virtually the entire field range up to 1.4 tesla where the last vestiges of superconductivity vanish. It can do so through the formation of flux vortices inherent to type II superconductivity. A more or less gradual rise in inductance thereby results as the flux density within the core particles builds. Only at very low fields is the inductance unaffected by changes in the dc field. Here the behavior stems basically from the same mechanism as that encountered in the lead-filled sample.

Briefly, the irregular shape of the particles causes the dc field to penetrate at applied fields well below the lower critical field H_{c1}, the limit for the Meissner state in type II materials. The particles thus assume a multiply connected structure as visualized for the lead sample. And as previously discussed, the particles experience total shielding from the ac field only so long as the eddy currents are wholly superconducted. The departure of the inductance curve from its zero field base line near 0.03 tesla marks the onset of ac field penetration. As will be shown, this coincides with the criterion for breakdown of the superconducting network at 0.5 H_{c1}.

A value of 0.058 tesla (580 G) for H_{c1} can be established on the basis of the Ginzburg-Landau κ value derived from the inductance curve. To do this, identify the abrupt change in the inductance just above 0.8 tesla with the transition of the bulk to the normal state at the upper critical field H_{c2}. Then, using a value of 0.155 tesla (ref. 15) for the thermodynamic critical field at 4.2 K, and taking $H_{c2} = 0.83$ tesla, calculate

$$\kappa = \frac{H_{c2}}{\sqrt{2}\ H_c} = 3.8 \tag{5}$$

Alternately, the saturation of the conductance and/or inductance at 1.4 tesla may be identified with the surface critical field H_{c3}. Then one might calculate κ using equation (4). The two results are consistent.

Thus, having obtained a credible value for κ, it is possible to stipulate a value for H_{c1}. However, one must be careful to recognize that the often quoted relation

$$\frac{H_{c1}}{H_c} = \frac{1}{\sqrt{2}\,\kappa}(\ln \kappa + 0.08) \tag{6}$$

applies only to type II materials with κ well above 1. In contrast to the situation for high κ materials, the magnetic energy contained in the core of a low κ material cannot be neglected. Harden and Arp (ref. 16) have determined, by computer calculation, the ratio H_{c1}/H_c to within 1 percent for an arbitrary κ. Using their result that $H_{c1}/H_c = 0.371$ for $\kappa = 3.8$, the 0.058 tesla figure for H_{c1} follows directly.

In summary then, the three distinct field regions of the inductance curve are directly related to the size of the Ginzburg-Landau κ parameter. These regions are (1) the initial total shielding region, extending to $0.5\,H_{c1}$; (2) the intermediate region, extending to H_{c2}, in which the flux penetration builds to nearly total saturation; and (3) the region between H_{c2} and H_{c3} wherein only slight shielding exists via surface superconductivity.

The loss component of the impedance is reflected in the shunting conductance shown in figure 6(b). The rationale for presenting the loss in terms of a conductance is based on the fact that the test coil is driven by a constant voltage source. Hence, the shunting conductance is directly proportional to the power loss ($1/R = P/V^2$). In this way, the relative magnitudes of the various power losses in the core and in the copper windings and shield can be readily assessed.

Traditionally, attempts to describe the alternating-current losses in type II superconductors (refs. 17 to 21) have conformed, in general, to searches for the appropriate exponent in expressions of the form $P = H^n$. These attempts have had only isolated success in limited field regions. One attempt, more fundamentally based, adequately explains the field-dependent power loss in this sample. Based on the premise that a local variation in the field stimulates a local supercurrent at a density equal to the intrinsic critical current density $J_c(H)$, Bean (ref. 22) and London (ref. 23) formulated a theory for the alternating-current loss in type II superconductors. They argued that if the local current density induced by an increasing magnetic field is limited to $J_c(H)$, the field would progressively penetrate the bulk of the superconductor. As the shielding by supercurrents near the surface fails to screen the field, more and more of the superconductor is driven to carry shielding currents at the critical current density. When the applied field is subsequently reduced to zero, the superconductor retains a remnant flux from these supercurrents. By reversing the applied field and continuing it through a complete cycle, it can be shown that the superconductor traces a complete hysteresis loop.

If the amplitude of the ac field is sufficiently small so as not to totally penetrate the superconductor, and if the critical current density can be considered constant within the cycle, then a simple loss expression results. The energy loss per cycle, corresponding to the area of the hysteresis loop, is of the form

$$P = K \frac{H_m^3}{J_c(H)} \tag{7}$$

The quantity K is a constant which depends on the specific shape of the superconductor (i.e., the core particles in these tests), and H_m is the amplitude of the ac field. Since the ac fields used in these tests were extremely small, the approximation that $J_c(H)$ is constant throughout a cycle is valid.

To examine the superconducting loss in the niobium-filled core in terms of this theory requires that it first be isolated from the total power loss. Because of the complex interplay of the currents in the core, the shield, and the coil, this may be done only to a fair approximation. However, the approximations can be justified, and the result shows that the losses are in agreement with the Bean-London theory throughout the entire field region below H_{c2}.

The primary dissipative sources in the coil-shield combination chosen for these test samples are fourfold. There is first the resistive I^2R loss in the coil by the radiofrequency exciting current. Secondly, there is a resistive loss in the copper shield due to eddy currents induced therein. Third, there is a loss from the eddy currents induced in nonsuperconducting regions in the core particles; though this effect is small when the particles are small in comparison with the radiofrequency skin depth, nonetheless, it cannot be neglected. The fourth source of loss is that associated with the hysteresis in the superconducting regions of the core particles.

As developed in appendix B, each of these four sources can be expressed in terms of an equivalent shunting conductance. The measured conductance is the sum of these various conductances:

$$\frac{1}{R_{app}} = \frac{1}{R_{sc}} + \frac{1}{R_{norm}} + \frac{1}{(\omega L_{app})^2} \left[R_w + R_s \frac{M^2(0)}{L_s^2(0)} \left(\frac{1 - \sigma}{1 - c\sigma} \right)^2 \right] \tag{8}$$

Contained in the bracketed term are the copper losses of the coil windings and of the shield. The losses originating within the core (i.e., the normal rf skin loss and the superconducting loss) are listed separately as $1/R_{norm}$ and $1/R_{sc}$, respectively. To extract the superconducting alternating-current loss from the total loss requires a knowledge of the other dissipative sources and how they vary with field. This is made difficult by the fact that it is not possible to make separate measurements of either the coil winding resistance R_w nor of the shield resistance R_s. Any such attempt significantly distorts the current distributions within both the winding and the shield from those which would otherwise exist. The resistance of each element is an integrated effect dependent on the current distribution in that element. Thus, it is necessary to make measurements

keeping the shield in place around the coil. Table III lists a series of conductance measurements made both with the niobium core in place and with it removed. These measurements permit one to separate the contributions to the total power loss by the various dissipative sources.

TABLE III. - SHUNTING CONDUCTANCE OF NIOBIUM

SAMPLE COIL ASSEMBLY AT 4.2 K

	Magnetic field, H, T	Apparent loss $1/R_{app}$, μmho
Shielded coil, core removed	1.4	204
Shielded coil, with core	1.4 0	237 420

The technique here is to realize that the superconducting loss is zero both above 1.4 tesla and at $H = 0$. Above 1.4 tesla, of course, the core is totally normal. At $H = 0$ the critical current density $J_c(H)$ becomes extraordinarily large. Hence, with the power loss proportional to $1/J_c(H)$ according to the Bean-London theory, the loss vanishes here too. Then, from the conductances measured at 1.4 tesla ($\sigma = 0$) both with and without the core (i.e., 237 and 204 μmho, respectively), the normal radiofrequency loss for total radiofrequency field penetration may be obtained directly as their difference, 33 μmho. These figures together with the sample conductance of 420 μmho measured at zero field where both $1/R_{sc} = 0$ and $1/R_{norm} = 0$ provide sufficient information to calculate the winding and shield resistance terms. Lumping the field independent quantities with R_w and R_s as constants a_1 and a_2 gives the total core loss as

$$\frac{1}{R_{core}(H)} = \frac{1}{R_{app}(H)} - \frac{1}{L_{app}^2(H)} \left\{ a_1 + a_2 \left[\frac{1 - \sigma(H)}{1 - c\sigma(H)} \right]^2 \right\} \tag{9}$$

where $a_1 = 385\ \mu\text{mho}\cdot\mu H^2$, $a_2 = 128\ \mu\text{mho}\cdot\mu H^2$, and $\sigma(H)$ is the superconducting filling factor of figure 6(c). The parameter c is determined by that fraction of radiofrequency flux, generated inside the shield by shield currents which actually links the coil (see appendix B); $c = 0.247$ for the configuration used in the test sample. The total core loss curve shown in figure 7 was constructed using this expression.

In the same figure is a curve for the loss from the normal radiofrequency eddy cur-

rents in the core. The assumption is made that the normal radiofrequency power loss may be expressed as the product of an average resistivity, an effective eddy current density, and the normal fraction of core volume:

$$P_{norm}(H) = \text{Constant} \times J^2_{norm}(H) \left[1 - \frac{\sigma(H)}{\sigma(0)}\right] \tag{10}$$

The resistivity of the particles to the normal radiofrequency currents is included in the constant. The eddy current density can be shown, through its relation to the radiofrequency field, to be directly proportional to the radiofrequency coil current. And since the impedance of the sample is almost entirely reactive, the coil current and thus J_{norm} vary inversely with the apparent sample inductance L_{app}. The radiofrequency power can, therefore, be approximated by

$$P_{norm}(H) = \text{Constant} \times \frac{1}{L^2_{app}(H)} \left[1 - \frac{\sigma(H)}{\sigma(0)}\right] \tag{11}$$

Normalizing this equation by the power loss measured at 1.4 tesla and expressing the result as an equivalent shunting conductance, one obtains

$$\frac{1}{R_{norm}(H)} = \frac{1}{R_{norm}(1.4\ T)} \frac{L^2_{app}(1.4\ T)}{L^2_{app}(H)} \left[1 - \frac{\sigma(H)}{\sigma(0)}\right] \tag{12}$$

The normal radiofrequency curve of figure 7 was plotted using this expression. The difference in conductance between the two curves in figure 7 is then the conductance $1/R_{sc}(H)$ representing the superconducting loss.

It remains only to relate the field dependency of the superconducting loss to the critical current density $J_c(H)$. On the basis of the Bean-London theory, the specific power loss (loss per unit volume of superconductor) is of the form H^3_m/J_c. Thus, the superconductive loss may be approximated by

$$P_{sc}(H) = \text{Constant} \times \frac{H^3_m}{J_c(H)} \sigma(H) \tag{13}$$

where H_m is the radiofrequency field amplitude averaged over the core volume. Since the radiofrequency is proportional to the coil current and, as previously argued, thereby inversely proportional to the sample inductance, the superconductive loss may be written

$$\frac{1}{R_{sc}(H)} = \text{Constant} \times \frac{\sigma(H)}{L_{app}^3(H)J_c(H)} \tag{14}$$

The use of this expression requires a knowledge of the critical current density $J_c(H)$. A reliable measurement of $J_c(H)$ for the powder particles was not possible. However, there is such data available on niobium with a similar κ (ref. 24). Using that data, a comparison of the observed loss against the functional form of equation (14) is possible. Shown in figure 8 is a logarithmic cross plot of the quantity $L_{app}^3(H)/R_{sc}(H)\sigma(H)$ against the published data for $J_c(H)$. The entire field range up to H_{c2} (the limit of the Bean-London theory) is covered. The fit of the data to the straight line with a slope approximately equal to -1 is in agreement with the theory.

As the applied field is raised to the upper critical field H_{c2}, the core enters a region of rapidly changing conductivity as the filamentary structure of the superconducting mixed state is destroyed. Simultaneously, the ac field is seen to approach nearly complete penetration. That this condition gives rise to a peak in the power dissipation was discussed in conjunction with the lead-filled sample. The mechanism is basically the same in both cases. The two cases differ only in that superconducting regions can exist in a niobium particle above H_{c2} at its surface. Complete penetration of the field is, therefore, retarded. The field region over which the power loss exists extends to an applied field of magnitude H_{c3}. As for the lead, a functional dependence of the loss term on field could not be found due to the complexity of the system.

No hysteresis effect was observed in the response of the niobium-filled sample to dc fields sequenced in opposite directions. The absence of any such effect is in contrast to the hysteresis seen in the lead-filled sample. It is, however, reasonable that the niobium would show no such effect. Nucleation of the superconducting state occurring at the surface at H_{c3} is initiated well above the bulk critical field H_{c2}. Thus, it matters not to the response from which direction a particular field is approached; the propagation of the superconducting state throughout the bulk never suffers a lack of nucleation since $H_{c3} > H_{c2}$.

Hysteresis might have been expected on the basis of the irreversibility in the magnetization for which cold worked type II superconductors are notorious. However, it has been observed repeatedly that the ac susceptibility is not simply the field derivative of the magnetization dM/dH (refs. 25 and 26) (i.e., the slope of the dc magnetization curve). Instead, it is observed that the superconductor responds in a nearly perfect diamagnetic and reversible fashion to small field excursions (refs. 27 and 28). Hitchcock (ref. 15) showed how a pseudoreversible magnetization curve could, in fact, be generated through recognition of this fact. Similarly, the response of the superconducting regions in the core particles to the small radiofrequency field is also a locally reversible diamagnetic response.

CONCLUDING REMARKS

This work is a preliminary investigation of the capabilities and limitations of superconductive dust cores. One of its aims was to determine to what extent the dust cores affect the impedance of an inductive coil. The other was to develop an understanding of the mechanisms involved.

The results show that the superconducting regions in the core shield those regions in a perfectly diamagnetic fashion from the small ac field. In addition, they show that the inductance is governed directly by the percentage of superconducting material in the core. Conceivably then, one could achieve any desired ratio of inductances by properly adjusting the filling factor. This might also include the distribution of superconducting particles throughout the windings of a multilayer coil.

The alternating-current losses in the core represent the most serious limitation. Aside from the normal eddy current losses, there are significant losses associated with the superconducted currents. The "superconducting" loss is seen to originate in two distinct ways. One way, common to both classes of superconductors, is through the shielding currents being driven in part through normally conducting regions. These losses are greatest as the inductance approaches saturation. The second loss mechanism is unique to the mixed state of type II superconductors. The loss here arises from a small hysteretic response to the ac field. It is related to the dc critical current density throughout the entire field region below the upper critical field, as theorized by Bean and London.

The resistive losses from normal eddy currents can be kept to a minimum. Only at frequencies where the skin depth is smaller than the particle sizes do the losses assume overwhelming proportions. The allowable particle sizes for a particular application are thus limited by the intended upper frequency.

As regards the total behavior of both core types, the magnitude of the Ginzburg-Landau parameter κ is crucial. In the lead-filled sample, the hysteresis-like response is directly related to the fact that κ is 0.39, permitting "supercooling" to occur. In the niobium-filled sample, κ relates the three fields at which the inductance (1) begins to increase, (2) approaches saturation, and (3) finally attains saturation, to the three critical fields H_{c1}, H_{c2}, and H_{c3}.

Lewis Research Center,
National Aeronautics and Space Administration,
Cleveland, Ohio, January 6, 1969,
129-02-05-10-22.

APPENDIX A

MEASUREMENT OF IMPEDANCES THROUGH TRANSMISSION LINES

For a variety of reasons, testing of circuit elements or devices may require that they be remotely located during the test. For example, the test may require special environmental conditions. In these instances one must allow for the perturbing effect of the interconnecting transmission line on the measurement.

Frequently, the assumption is made that the line can be replaced by a pi or tee equivalent representation. Unfortunately, this can generate a significant error. Also, ignoring the finite attenuation of the line can generate a sizable error. It is possible, however, to deal totally and exactly with the perturbing effect of an arbitrary length of transmission line (losses included). It simply requires noting the apparent line impedances with the unknown element replaced (1) with an open circuit then (2) with a short circuit.

This technique is based on the following. An unknown impedance Z_x mounted at one end of a transmission line is seen at the opposite end of the line as an apparent impedance Z_x' (sketch a):

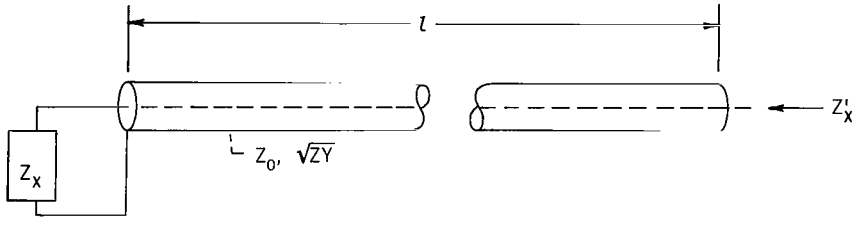

(a)

The two are related by (ref. 29):

$$Z_x' = Z_o \frac{\left(\frac{Z_x}{Z_o}\right)\cosh\sqrt{ZY}\, l + \sinh\sqrt{ZY}\, l}{\cosh\sqrt{ZY}\, l + \left(\frac{Z_x}{Z_o}\right)\sinh\sqrt{ZY}\, l} \tag{A1}$$

Z_o is the characteristic impedance of the line, $\sqrt{ZY}$ is the propagation constant (which includes line losses), and l is the length of the line. With the line open-circuited

(i.e., $Z_x = Z_{op} = \infty$), the impedance seen at the other end of the line is

$$Z'_{op} = \frac{Z_o}{\tanh\sqrt{ZY}\ l} \tag{A2}$$

With a short-circuited load (i.e., $Z_x = Z_{sh} = 0$), the observed impedance is

$$Z'_{sh} = Z_o \tanh\sqrt{ZY}\ l \tag{A3}$$

The transformed impedance of an unknown load can thus be expressed in terms of the observable open- and short-circuit impedances:

$$Z'_x = \frac{Z_x + Z'_{sh}}{1 + \left(\frac{Z_x}{Z'_{op}}\right)} \tag{A4}$$

Alternately, the actual impedance of the unknown can be extracted as

$$Z_x = \frac{Z'_x - Z'_{sh}}{1 - \left(\frac{Z'_x}{Z'_{op}}\right)} \tag{A5}$$

The convention adopted herein is to label all quantities measured at the accessible end of the transmission line with a prime; the actual impedances at the remote end are unprimed.

For low-loss elements it is often more convenient to think in terms of equivalent admittances. In this frame of reference, equation (A5) can be restated as

$$\frac{1}{Z_x} = \frac{\left(\frac{1}{Z'_x}\right) - \left(\frac{1}{Z'_{op}}\right)}{1 - \left(\frac{Z'_{sh}}{Z'_x}\right)} \tag{A6}$$

In an actual measurement, Z'_x, Z'_{op}, and Z'_{sh} are specified by their equivalent shunting conductances and inductances as

$$\frac{1}{Z'_x} = \frac{1}{R'_x} - j\frac{1}{\omega L'_x} \tag{A7}$$

$$\frac{1}{Z'_{op}} = \frac{1}{R'_{op}} - j\frac{1}{\omega L'_{op}} \tag{A8}$$

$$\frac{1}{Z'_{sh}} = \frac{1}{R'_{sh}} - j\frac{1}{\omega L'_{sh}} \tag{A9}$$

It is easily shown that the ratio Z'_{sh}/Z'_x has a magnitude

$$\left|\frac{Z'_{sh}}{Z'_x}\right| = \frac{L'_{sh}}{L'_x}\left[1 + \frac{1}{(Q'_{sh})^2}\right]^{-1/2}\left[1 + \frac{1}{(Q'_x)^2}\right]^{1/2} \tag{A10}$$

and has a phase angle θ given by

$$\theta = \tan^{-1}\left(\frac{Q'_{sh} - Q'_x}{1 + Q'_{sh}Q'_x}\right) \tag{A11}$$

where the quality factors Q'_x and Q'_{sh} for the unknown and short-circuited lines, respectively, are defined according to

$$Q'_x = \frac{R'_x}{\omega L'_x} \tag{A12}$$

and

$$Q'_{sh} = \frac{R'_{sh}}{\omega L'_{sh}} \tag{A13}$$

For low-loss elements and line $(Q'_x)^2 >> 1$ and $(Q'_{sh})^2 >> 1$. The expression for the admittance of the unknown load thus reduces to

$$\frac{1}{Z_x} = \frac{\frac{1}{Z'_x} - \frac{1}{Z'_{op}}}{1 - \frac{L_{sh}}{L'_x} e^{j\theta}} \tag{A14}$$

Thus, the individual shunting inductance and conductance are obtained as

$$L_x = L'_x \frac{1 - 2\alpha \cos\theta + \alpha^2}{(1 - \beta)(1 - \alpha \cos\theta) - \frac{1}{Q'_x}(1 - \gamma)\alpha \sin\theta} \tag{A15}$$

and

$$\frac{1}{R_x} = \frac{1}{R'_x} \frac{(1 - \gamma)(1 - \alpha \cos\theta) + Q'_x(1 - \beta)\alpha \sin\theta}{1 - 2\alpha \cos\theta + \alpha^2} \tag{A16}$$

The parameters α, β, and γ are defined as

$$\alpha = \frac{L'_{sh}}{L'_x} \tag{A17}$$

$$\beta = \frac{L'_x}{L'_{op}} \tag{A18}$$

$$\gamma = \frac{R'_x}{R'_{op}}$$

APPENDIX B

ANALYSIS OF SHIELDED COILS WITH VARIABLE CORES

Conceptually, an inductive coil inside an electrostatic shield is like a transformer with a shorted single turn secondary. The coil behaves as the primary, the shield as the secondary. Between the two exists a mutual inductive coupling. Thus, an analysis of the shielded coil can be made on the basis of its similarity to the shorted transformer.

By analogy then, the coil, as represented in sketch b, is an inductance L_w in series with a winding resistance of R_w. The shield is represented as an inductance L_s with an effective resistance R_s. Inductive coupling between the coil and shield is indicated by a mutual inductance M. A shunting resistance R_c was included across the coil's terminals to account for losses originating in the core.

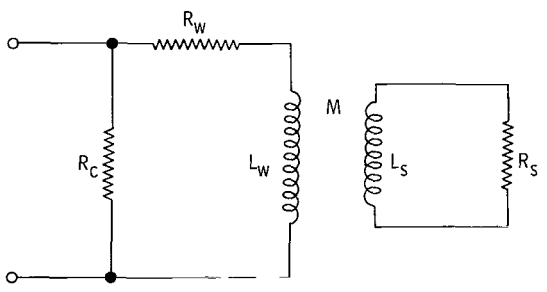

(b)

It is readily shown that the shield reduces the inductance of the coil to an effective value

$$L_{eff} = L_w \left[1 - k^2 \left(\frac{1}{1 + \frac{1}{Q_s^2}} \right) \right] \tag{B1}$$

The mutual coupling coefficient k^2 is

$$k^2 = \frac{M^2}{L_w L_s} \tag{B2}$$

and the quality factor of the shield Q_s is defined at the angular frequency ω as

$$Q_s = \frac{\omega L_s}{R_s} \tag{B3}$$

The shield also effectively raises the series resistance to

$$R_{eff} = R_w \left[1 + \left(\frac{R_s}{R_w} \right) \left(\frac{L_w}{L_s} \right) k^2 \left(\frac{1}{1 + \frac{1}{Q_s^2}} \right) \right] \tag{B4}$$

Accordingly, the Q of the shielded coil is degraded to

$$Q_{eff} = \frac{\omega L_{eff}}{R_{eff}} \tag{B5}$$

Up to this point the core losses represented by R_c have been neglected. To include them it is convenient to first express the effective inductance and resistance of the shielded coil in terms of their equivalent parallel components. Then the total impedance of the shielded coil (including core losses) is an apparent inductance

$$L_{app} = L_{eff} \left(1 + \frac{1}{Q_{eff}^2} \right) \tag{B6}$$

shunted by an apparent conductance

$$\frac{1}{R_{app}} = \frac{1}{R_c} + \frac{1}{R_{eff}} \left(\frac{1}{1 + Q_{eff}^2} \right) \tag{B7}$$

Ordinarily, one would not deliberately operate the coil at a frequency at which it would be lossy. Rather, one would ensure that the impedance was predominantly reactive. Then both Q_{eff}^2 and Q_s^2 are sufficiently large to allow simplifying approximations

in equations (B6) and (B7). The resulting error is negligible. After some algebraic manipulations the apparent inductance and shunting conductance become

$$\left(L_{app}\right)_{\substack{Q_{eff}^2>>1 \\ Q_s^2>>1}} = L_w(1 - k^2) \tag{B8}$$

and

$$\left(\frac{1}{R_{app}}\right)_{\substack{Q_{eff}^2>>1 \\ Q_s^2>>1}} = \frac{1}{R_c} + \frac{1}{(\omega L_{app})^2}\left[R_w + R_s\left(\frac{M}{L_s}\right)^2\right] \tag{B9}$$

Now, with a core of variable susceptibility, the several quantities in these expressions become field dependent. Unfortunately, field induced variations in the superconducting filling factor not only affect the inductance and conductance, but also the inductive and resistive loading of the coil by the shield. This arises through the changes in the inductive coupling between the coil and shield. However, through the flux-related definition for inductance, the field dependence can be formulated in terms of the superconducting filling factor. In what follows, the flux referred to is understood to be only that ac component generated in the axial direction of the coil.

The self-inductance of the coil L_w may be expressed in terms of the superconducting filling factor as

$$L_w = \frac{\partial\varphi_w(\sigma)}{\partial I_w} = \frac{\partial\varphi_w(0)}{\partial I_w}(1 - \sigma) = L_w(0)(1 - \sigma) \tag{B10}$$

where $L_w(0)$ is the self-inductance with a totally normal core (i. e., $\sigma = 0$). Similarly, the mutual inductance M may be expressed as

$$M = N\frac{\partial\varphi_w(\sigma)}{\partial I_s} = N\frac{\partial\varphi_w(0)}{\partial I_s}(1 - \sigma) = M(0)(1 - \sigma) \tag{B11}$$

where $M(0)$ is the mutual inductance existing with a totally normal core and N is the

number of turns in the coil. Finally, the self-inductance of the shield may be expressed as the sum of two components, one dependent on σ, the other independent of σ:

$$L_s = \frac{\partial \varphi_s(\sigma)}{\partial I_s} = \frac{\partial}{\partial I_s}\left[\varphi_w(\sigma) + \varphi'\right] = \frac{M(0)}{N}(1 - \sigma) + \frac{\partial \varphi'}{\partial I_s} \tag{B12}$$

Here, $\varphi_w(\sigma)$ is the flux contained within the coil, and φ' is the flux produced in the space between the shield and the coil. The field independent component is a constant which can be evaluated as

$$\frac{\partial \varphi'}{\partial I_s} = L_s(0) - \frac{M(0)}{N} \tag{B13}$$

Therefore, the mutual coupling coefficient k^2, as given by equation (B2), becomes

$$k^2 = \frac{M^2(0)(1 - \sigma)}{L_w(0) \cdot L_s(0)\left[1 - \frac{M(0)}{NL_s(0)}\sigma\right]} \tag{B14}$$

Using the definitions for $M(0)$ and $L_s(0)$ as given in equations (B11) and (B12), it is readily apparent that the quantity

$$\frac{M(0)}{NL_s(0)} = \frac{\dfrac{\partial \varphi_w(0)}{\partial I_s}}{\dfrac{\partial \varphi_s(0)}{\partial I_s}} = c \tag{B15}$$

is a constant for a given coil-shield combination. Its value specifies the fraction of the flux generated within the shield by shield currents that exists inside the totally normal core. The mutual coupling coefficient can thus be written as

$$k^2 = k_o^2\left(\frac{1 - \sigma}{1 - c\sigma}\right) \tag{B16}$$

where k_o^2, defined according to

$$k_o^2 = \frac{M^2(0)}{L_w(0)L_s(0)} \tag{B17}$$

is its value for a totally normal core. Therefore, it follows that the apparent inductance of the shielded coil containing the magnetically variable core is

$$\left(L_{app}\right)_{\substack{Q_{eff}^2>>1 \\ Q_s^2>>1}} = L_w(0)(1 - \sigma)\left[1 - k_o^2\left(\frac{1 - \sigma}{1 - c\sigma}\right)\right] \tag{B18}$$

and the shunting conductance is

$$\left(\frac{1}{R_{app}}\right)_{\substack{Q_{eff}^2>>1 \\ Q_s^2>>1}} = \frac{1}{R_c} + \frac{1}{(\omega L_{app})^2}\left\{R_w + R_s\left[\frac{M^2(0)}{L_s^2(0)}\right]\left(\frac{1 - \sigma}{1 - c\sigma}\right)^2\right\} \tag{B19}$$

It remains only to evaluate the constant c in these expressions. This may be done by separately evaluating the mutual inductance M(0) and the shield inductance $L_s(0)$, and then using those values to calculate the constant c according to equation (B15). The mutual inductance between the coil and the shield is similar to that developed between two coaxial cylindrical current sheets. The outer current sheet corresponds to the induced shield current, and is assumed to have the same axial length as the inner current sheet representing the coil. This is a reasonable assumption since the eddy currents are induced essentially only in the immediate vicinity of the coil. Thus, based on an equation given by Grover (ref. 5, p. 128), the mutual inductance M(0) may be calculated using

$$M(0)[\mu H] = 0.0005\,\pi^2\left(\frac{d_w}{l_w}\right)^2 N d_s[cm]\left[\sqrt{1 + \left(\frac{2l_w}{d_s}\right)^2}\,B_1 - B_2\right] \tag{B20}$$

where B_1 and B_2 are tabulated functions (ref. 5, pp. 124-126) dependent upon the dimensions of the coil and shield.

The self-inductance of the shield may be obtained as that of a cylindrical current sheet having the same diameter as the shield and with a length equal to that of the coil. From an equation given by Grover (ref. 5, p. 143),

$$L_s(0)[\mu H] = 0.002\ \pi d_s[cm]\left[\log_e\left(\frac{4d_s}{l_w}\right) - \frac{1}{2}\right] \tag{B21}$$

Listed in table IV are the values for the constant c calculated using these expressions. As a check on these computations, k_o^2 calculated using M(0), $L_s(0)$, and the measured values of $L_w(0)$ are listed for comparison with k_o^2 derived from the empirical expression of Bogle (ref. 8). Also listed are values for k_o^2 obtained from the actual measurements of the shielded and unshielded coils. The agreement among the variously determined values lends credence to the calculated values for c.

TABLE IV. - INDUCTIVELY RELATED PARAMETERS

OF SAMPLE COILS

Parameter	Sample	
	Pb-815	Nb-815
Mutual inductance, M(0), by eq. (B20), μH	0.172	0.0713
Shielded inductance, $L_s(0)$, by eq. (B21), μH	0.0169	0.0141
Constant, $c = \frac{M(0)}{NL_s(0)}$	0.212	0.247
Normal mutual coupling coefficient, k_o^2:		
By eq. (B17)	0.135	0.178
By empirical calculation	0.137	0.166
By direct measurement	0.136	0.157

REFERENCES

1. Slade, Albert E.: Superconductive Switching Elements. U.S. Patent 2,946,030, 1960.
2. Cassidy, Carl R.; and Meyerhoff, Albert J.: Superconducting Controlled Inductance Circuits. U.S. Patent 3,275,930, 1966.
3. Grange, R. A.: The Ryotron - A New Cryogenic Device. Proc. IEEE, vol. 52, no. 10, Oct. 1964, pp. 1216-1223.
4. Miller, J. C.; Wine, C. M.; Cosentino, L. S.: The Ryotron - A Variable Inductance Cryogenic Device. Proc. IEEE, vol. 52, no. 10, Oct. 1964, pp. 1223-1233.
5. Grover, Frederick W.: Inductance Calculations, Working Formulas and Tables. Dover Publ., 1962.
6. Weast, Robert C., ed.: Handbook of Chemistry and Physics. 48 ed., Chemical Rubber Co., 1967-1968, p. B-118.
7. Harding, John T.: Density of Niobium. J. Appl. Phys., vol. 37, no. 2, Feb. 1966, p. 928.
8. Bogle, A. G.: Effective Inductance and Resistance of Screened Coils. J. IEE, vol. 87, no. 525, Sept. 1940, pp. 299-316.
9. Shoenberg, D.: Superconductivity. Second ed., Cambridge University Press, 1960, p. 23.
10. Saint-James, D.; and Gennes, P. G.: Onset of Superconductivity in Decreasing Fields. Phys. Letters, vol. 7, no. 5, Dec. 15, 1963, pp. 306-308.
11. Feder, J.: Comments on the Supercooling Field for Superconductors with Values Near 0.4. Solid State Comm., vol. 5, no. 4, Apr. 1967, pp. 299-301.
12. Park, J. G.: Metastable States of the Supercooling Surface Sheath in Decreasing Fields. Solid State Comm., vol. 5, no. 8, Aug. 1967, pp. 645-648.
13. McEvoy, J. P.; Jones, D. P.; Park, J. G.: Supercooling of Superconductors Below the Surface Nucleation Field. Solid State Comm., vol. 5, no. 8, Aug. 1967, pp. 641-644.
14. Strongin, Myron; Paskin, Arthur; Schweitzer, Donald G.; Kammerer, O. F.; and Craig, P. P.: Surface Superconductivity in Type I and Type II Superconductors. Phys. Rev. Letters, vol. 12, no. 16, Apr. 20, 1964, pp. 442-444.
15. Hitchcock, Harley C.: Pseudoreversible Magnetization of Nb. Rev. Mod. Phys., vol. 36, no. 1, pt. 1, Jan. 1964, pp. 61-64.

16. Harden, J. L.; and Arp, V.: The Lower Critical Field in the Ginzburg-Landau Theory of Superconductivity. Cryogenics, vol. 3, no. 2, June 1963, pp. 105-108.

17. Buchhold, T. A.; and Molenda, P. J.: Surface Electrical Losses of Superconductors in Low Frequency Fields. Cryogenics, vol. 2, no. 6, Dec. 1962, pp. 344-347.

18. Buchhold, T. A.: The Nature of the Surface Losses of Superconductors at Low Frequencies. Cryogenics, vol. 3, no. 3, Sept. 1963, pp. 141-149.

19. Lord, A. N.: Compositional Effects on Low Frequency, Low Field Power Losses in Columbium. J. Metals, vol. 16, no. 1, Jan. 1964, p. 90.

20. Rocher, Y. A.; and Septfonds, J.: Losses of Superconducting Niobium in Low Frequency Fields. Cryogenics, vol. 7, no. 2, Apr. 1967, pp. 96-102.

21. Victor, J. M.; Persyn, G. A.; and Rollwitz, W. L.: The Effect of Trapped Flux on RF Superconducting Losses. Cryogenics, vol. 7, no. 2, Apr. 1967, p. 119.

22. Bean, Charles P.: Magnetization of High-Field Superconductors. Rev. Mod. Phys., vol. 36, no. 1, pt. 1, Jan. 1964, pp. 31-39.

23. London, H.: Alternating Current Losses in Superconductors of the Second Kind. Phys. Letters, vol. 6, no. 2, Sept. 1, 1963, pp. 162-165.

24. Rosenblum, E. S.; Autler, S. H.; and Gooen, K. H.: The Dependence of the Upper Critical Field of Niobium on Temperature and Resistivity. Rev. Mod. Phys., vol. 36, no. 1, pt. 1, Jan. 1964, pp. 77-80, Sample no. 93.

25. Strongin, M.; and Maxwell, E.: Complex AC Susceptibility of Some Superconducting Alloys. Phys. Letters, vol. 6, no. 1, Aug. 15, 1963, pp. 49-51.

26. Goedemoed, S. H.; van der Giessen, A.; de Klerk, D.; and Gorter, C. J.: Magnetisation Curves in a Superconductor of the Second Kind. Phys. Letters, vol. 3, no. 5, Jan. 15, 1963, pp. 250-251.

27. Shoenberg, D.: Superconductors in Alternating Magnetic Fields. Proc. Cambridge Phil. Soc., vol. 33, 1937, pp. 559-575.

28. Park, J. G.: Superconducting Transition of Tin Alloys in an Alternating Field. Rev. Mod. Phys., vol. 36, no. 1, pt. 1, Jan. 1964, pp. 87-90.

29. Terman, Frederick Emmons: Radio Engineers' Handbook. McGraw-Hill Book Co., Inc., 1943, p. 183.

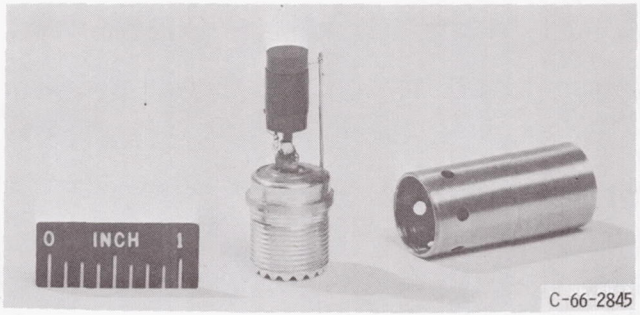

Figure 1. - Lead coil-core assembly with shield removed.

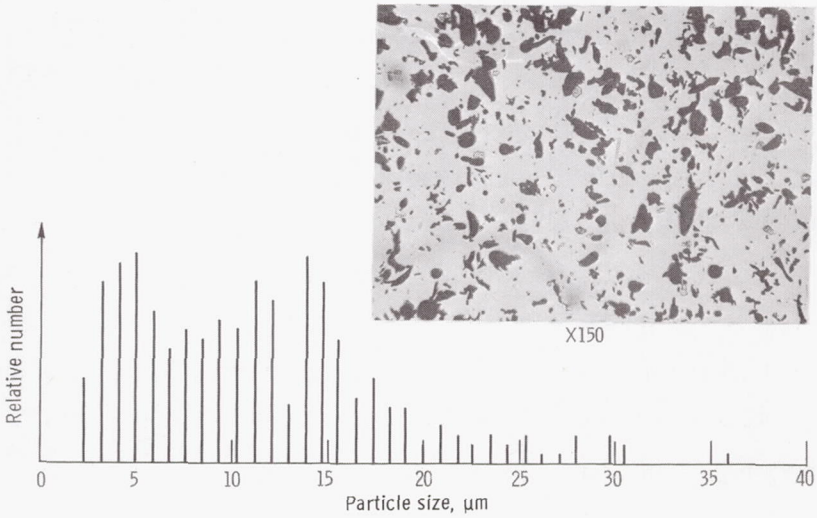

Figure 2. - Particle size distribution of lead dust.

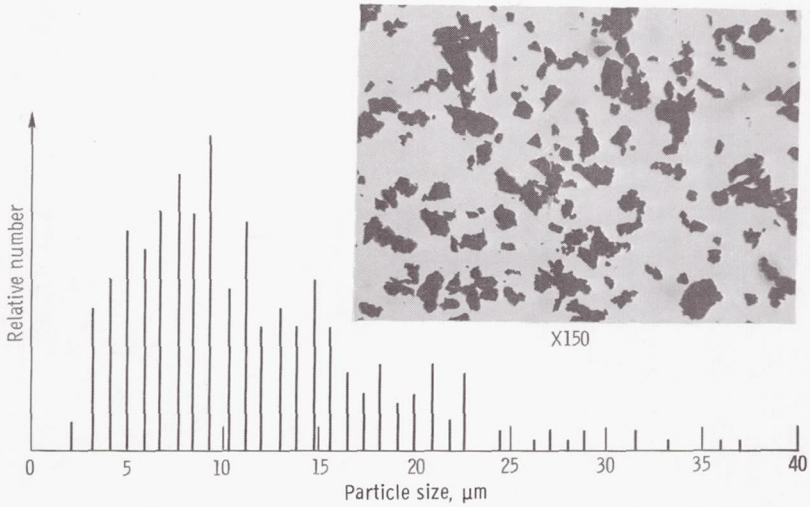

Figure 3. - Particle size distribution of niobium dust.

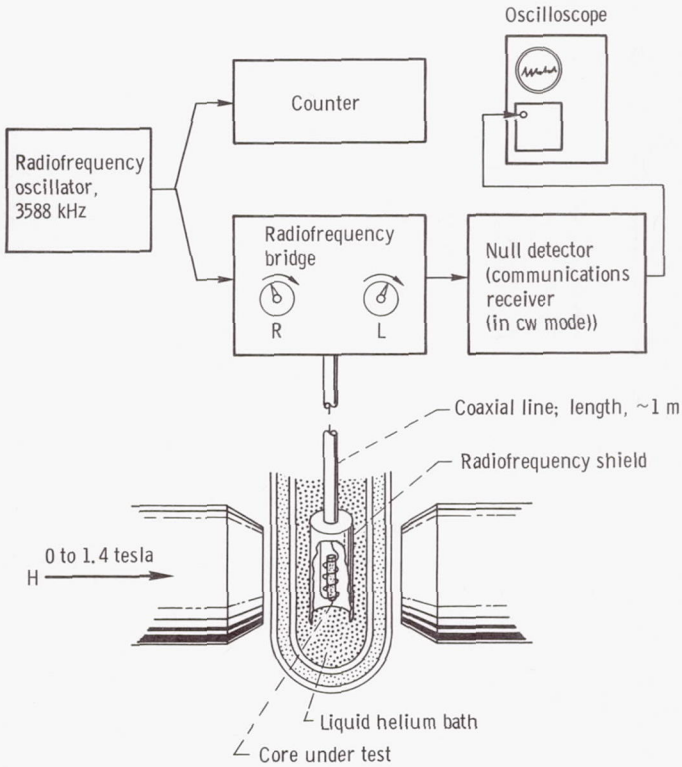

Figure 4. - Coil and core as tested at 3588 kilohertz.

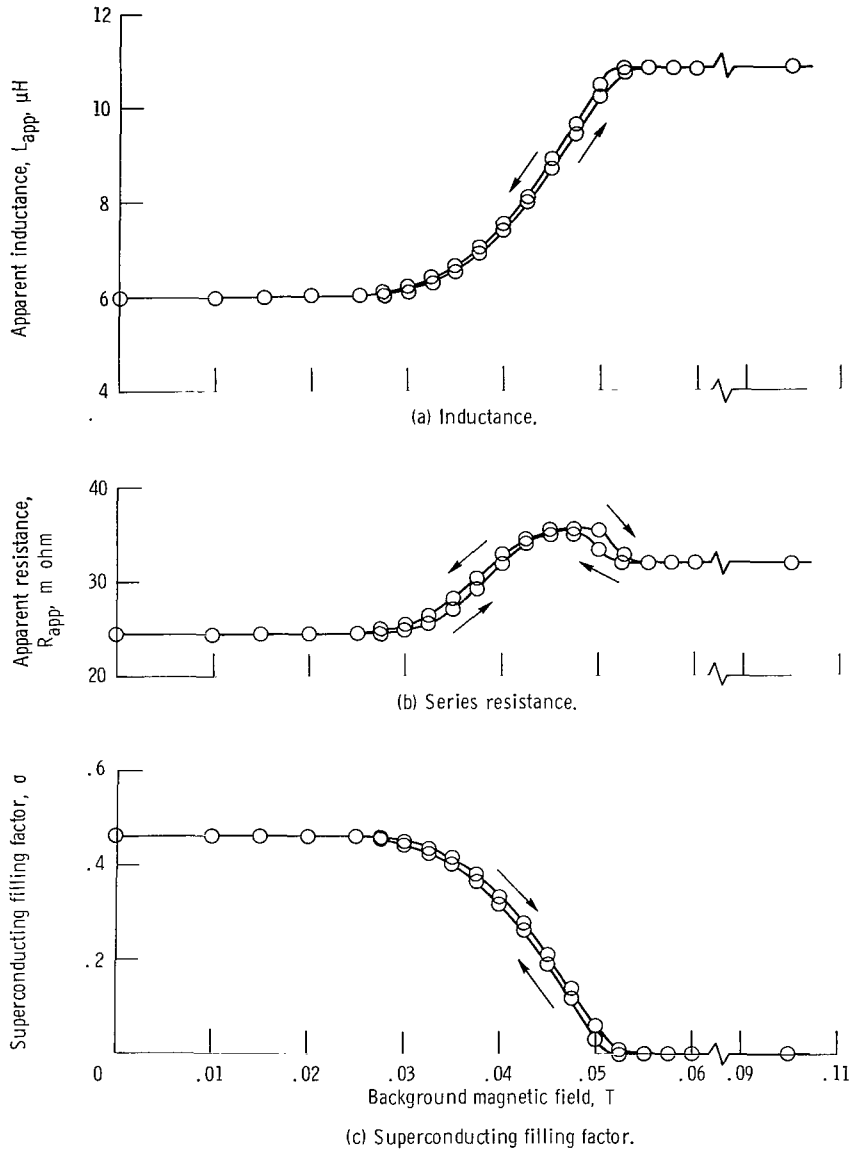

Figure 5. - Magnetic field properties of lead-filled sample. Temperature, 4.2 K; frequency, 10 kilohertz.

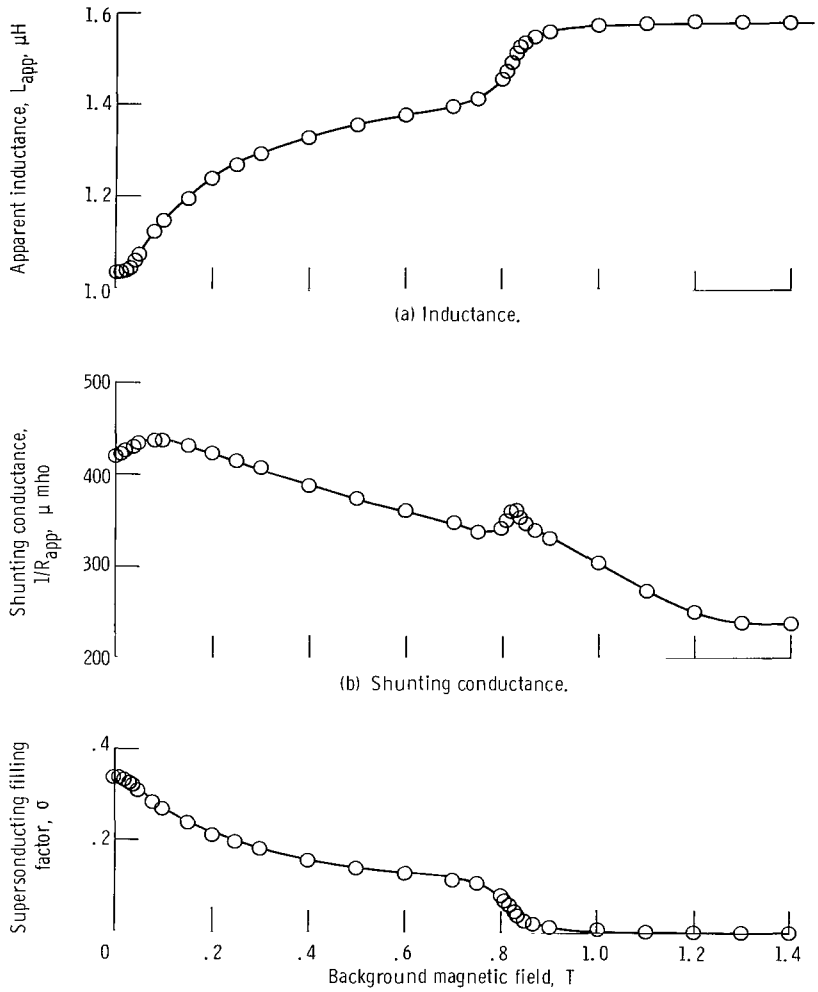

Figure 6. - Magnetic field properties of niobium-filled sample. Temperature, 4.2 K; frequency, 3588 kilohertz.

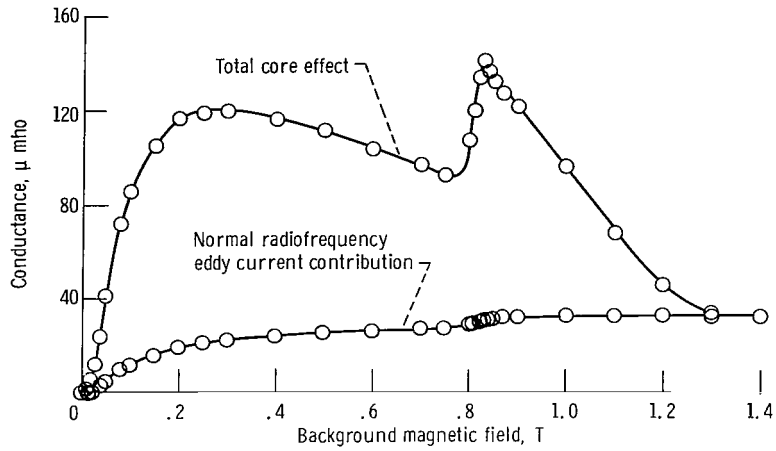

Figure 7. - Losses in Niobium-filled core. Temperature, 4.2 K; frequency, 3588 kilohertz.

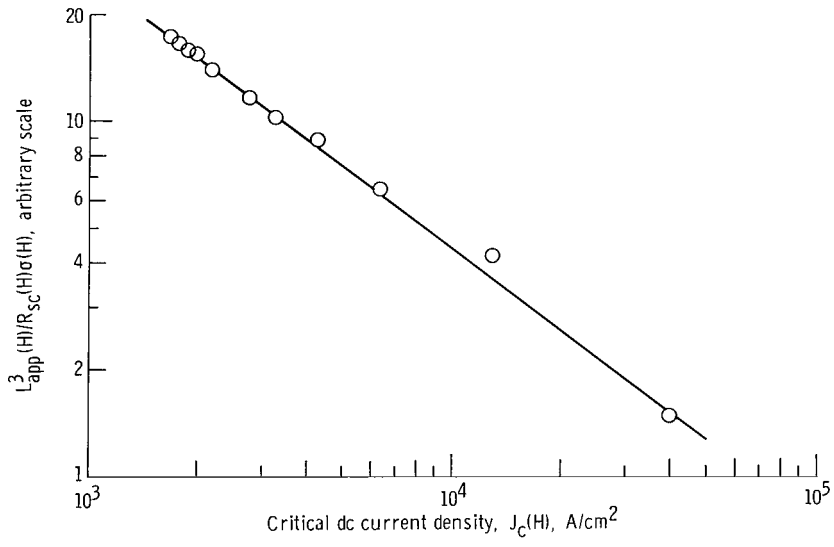

Figure 8. - Specific power loss in niobium-filled core according to Bean-London theory.

NASA-Langley, 1969 —— 26 E-4818

NATIONAL AERONAUTICS AND SPACE ADMINISTRATION
WASHINGTON, D. C. 20546

OFFICIAL BUSINESS

FIRST CLASS MAIL

POSTAGE AND FEES PAID
NATIONAL AERONAUTICS AND
SPACE ADMINISTRATION

POSTMASTER: If Undeliverable (Section 158 Postal Manual) Do Not Return

"The aeronautical and space activities of the United States shall be conducted so as to contribute . . . to the expansion of human knowledge of phenomena in the atmosphere and space. The Administration shall provide for the widest practicable and appropriate dissemination of information concerning its activities and the results thereof."

—NATIONAL AERONAUTICS AND SPACE ACT OF 1958

NASA SCIENTIFIC AND TECHNICAL PUBLICATIONS

TECHNICAL REPORTS: Scientific and technical information considered important, complete, and a lasting contribution to existing knowledge.

TECHNICAL NOTES: Information less broad in scope but nevertheless of importance as a contribution to existing knowledge.

TECHNICAL MEMORANDUMS: Information receiving limited distribution because of preliminary data, security classification, or other reasons.

CONTRACTOR REPORTS: Scientific and technical information generated under a NASA contract or grant and considered an important contribution to existing knowledge.

TECHNICAL TRANSLATIONS: Information published in a foreign language considered to merit NASA distribution in English.

SPECIAL PUBLICATIONS: Information derived from or of value to NASA activities. Publications include conference proceedings, monographs, data compilations, handbooks, sourcebooks, and special bibliographies.

TECHNOLOGY UTILIZATION PUBLICATIONS: Information on technology used by NASA that may be of particular interest in commercial and other non-aerospace applications. Publications include Tech Briefs, Technology Utilization Reports and Notes, and Technology Surveys.

Details on the availability of these publications may be obtained from:

SCIENTIFIC AND TECHNICAL INFORMATION DIVISION

NATIONAL AERONAUTICS AND SPACE ADMINISTRATION

Washington, D.C. 20546